

# $^{13}\text{C}$ and $^1\text{H}$ Magic-Angle-Spinning NMR Studies of the Conversion of Methanol over Offretite/Erionite Intergrowths

Michael W. Anderson,<sup>†,§</sup> Mario L. Occelli,<sup>†</sup> and Jacek Klinowski<sup>\*,†</sup>

Department of Chemistry, University of Cambridge, Lensfield Road, Cambridge CB2 1EW, U.K., and Science and Technology Division, Unocal Corporation, Brea, California 92621 (Received: May 16, 1991)

$^{13}\text{C}$  and  $^1\text{H}$  NMR with magic-angle spinning (MAS) has been used to monitor the conversion of methanol to low-molecular-weight hydrocarbons over intergrowths of the zeolites offretite and erionite with varying contents of the two structures. The sample richest in offretite shows the lowest selectivity to light olefins; this is correlated to the ease of formation of long-chain polymeric hydrocarbons within the intracrystalline space of offretite. The presence of such polymers is confirmed by  $^{13}\text{C}$  MAS NMR and we attribute it to the uninterrupted one-dimensional pore system. In erionite, where the channel system is constricted at every 15.2 Å, polymers cannot form. It appears that a degree of channel "tortuosity" is preferable in reactions which produce readily oligomerizable molecules, in order to prevent undesirable side reactions.

## Introduction

The coupling of  $\text{C}_1$  molecules to form  $\text{C}_2$  and higher molecular weight species is an important goal in the world of declining oil reserves. The starting point can be natural gas: synthesis gas ( $\text{CO} + \text{H}_2$ ) obtained from methane is converted to methanol ( $\text{MeOH}$ ) which reacts further to form light olefins.<sup>1</sup> Selective synthesis from  $\text{MeOH}$  of ethylene and propylene, the key intermediates for the production of detergents, plasticizers, lubricants, and a variety of chemicals, proceeds over smaller pore zeolites such as chabazite, offretite, and erionite.<sup>2-4</sup>

The related structures of the zeolites offretite and erionite (see Figure 1) readily intergrow,<sup>5,6</sup> so that an infinite variety of structures with varying contents of the two components can be synthesized. It has been shown<sup>7-9</sup> that it is possible to influence the degree of selectivity for the conversion of  $\text{MeOH}$  to light olefins by controlling the extent of the intergrowths, and that this effect is related to the degree of channel tortuosity.

We have demonstrated<sup>10-17</sup> that catalytic reactions on molecular sieves can be studied using in situ  $^{13}\text{C}$  and  $^1\text{H}$  MAS NMR, which monitors the species adsorbed in the intracrystalline space. NMR identifies a number of aliphatic and aromatic species in the adsorbed phase in the conversion of  $\text{MeOH}$  over zeolite H-ZSM-5, and monitors their fate during the course of the reaction. By using gas chromatography in tandem with NMR we have compared the composition of the adsorbed phase with that of the gaseous products leaving the catalyst. Although the conditions do not mimic exactly the conditions prevailing in a real reactor (the capsule is closed and contains excess methanol), valuable information about the catalytic process may be obtained from the spectra by keeping experimental conditions the same for both NMR and gas chromatography. We now describe the application of the technique to the conversion of  $\text{MeOH}$  over intergrowths of erionite and offretite. In what follows, we shall refer to the gaseous species leaving the catalyst (and monitored by gas chromatography) as "products" and the compounds monitored by NMR in the intracrystalline space as the "adsorbed phase".

## Experimental Section

**Catalyst Preparation.** Crystalline zeolites of the offretite-erionite type were synthesized using quaternary ammonium compounds as templates. Offretite (H-TMA-OFF) was prepared using the tetramethylammonium cation ( $\text{TMA}^+$ ).<sup>7</sup> Zeolite ZSM-34,

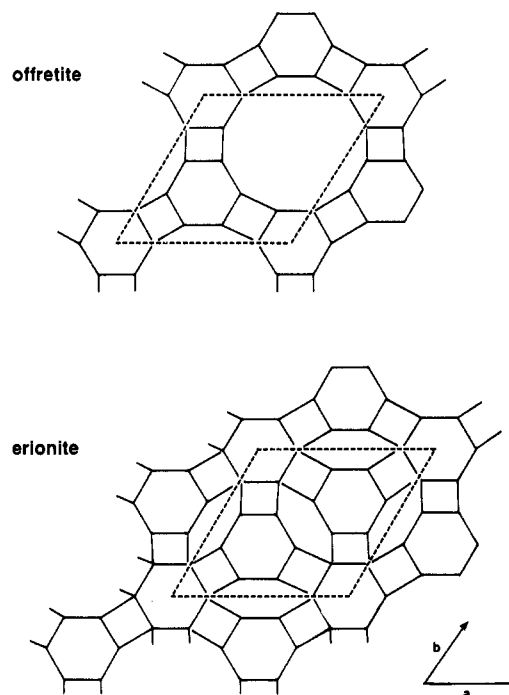


Figure 1. Structures of offretite and erionite looking down the  $c$  axis.

- (1) Maj, J. J.; Colmenares, C.; Somorjai, G. A. *Appl. Catal.* **1984**, *10*, 313.
- (2) Chang, C. D.; Lang, W. H.; Silvestri, A. J. U.S. Patent 4,062,905, 1978.
- (3) Singh, B. B.; Lin, F. N.; Anthony, R. G. *Chem. Eng. Commun.* **1980**, *4*, 749.
- (4) Wunder, F. A.; Leupold, E. I. *Angew. Chem., Int. Ed. Engl.* **1980**, *19*, 126.
- (5) Bennett, J. M.; Gard, J. A. *Nature* **1967**, *214*, 1005.
- (6) (a) Millward, G. R.; Ramdas, S.; Thomas, J. M. *Proc. R. Soc. London* **1985**, *A399*, 57. (b) Millward, G. R.; Thomas, J. M. *J. Chem. Soc., Chem. Commun.* **1984**, 77.
- (7) Occelli, M. L.; Innes, R. A.; Pollack, S. S.; Sanders, J. V. *Zeolites* **1987**, *7*, 265.
- (8) Sanders, J. V.; Occelli, M. L.; Innes, R. A.; Pollack, S. S. *New Developments in Zeolite Science and Technology. Proc. 7th Int. Zeolite Conf., Tokyo* **1986**, 429.
- (9) Occelli, M. L.; Ritz, G. P.; Iyer, P. S.; Walker, R. D.; Gerstein, B. C. *Zeolites* **1989**, *9*, 104.
- (10) Anderson, M. W.; Klinowski, J. *Nature* **1989**, *339*, 200.
- (11) Anderson, M. W.; Klinowski, J. *J. Am. Chem. Soc.* **1990**, *112*, 10.
- (12) Anderson, M. W.; Sulikowski, B.; Barrie, P. J.; Klinowski, J. *J. Phys. Chem.* **1990**, *94*, 2730.
- (13) Anderson, M. W.; Klinowski, J. *J. Chem. Soc., Chem. Commun.* **1990**, 918.

\* Address correspondence to this author.

<sup>†</sup> University of Cambridge.

<sup>‡</sup> Unocal Corporation.

<sup>§</sup> Present address: Department of Chemistry, UMIST, P.O. Box 88, Manchester M60 1QD, U.K.

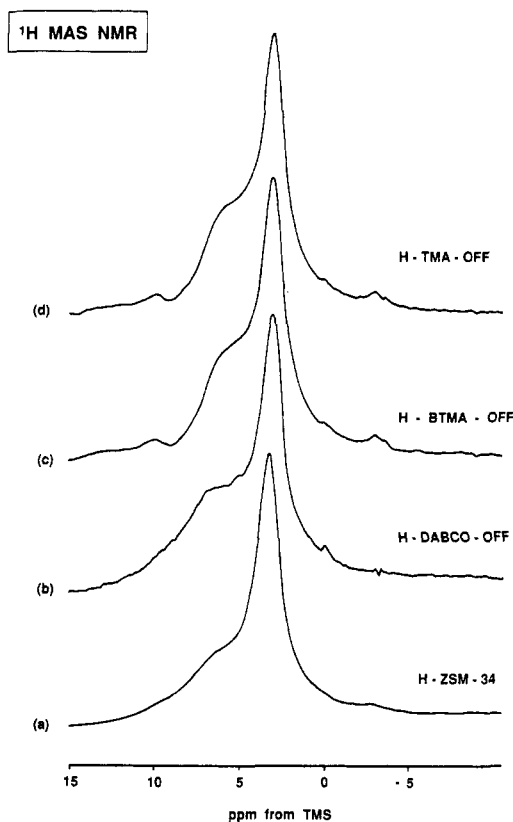


Figure 2.  $^1\text{H}$  MAS NMR spectra of methanol adsorbed on (a) H-ZSM-34; (b) H-DABCO-OFF; (c) H-BTMA-OFF; (d) H-TMA-OFF.

which has the structure of erionite, was synthesized using choline chloride (CC). Two intermediate erionite/offretite intergrowths were synthesized using 1,4-diazabicyclo[2.2.2]octane (DABCO) and benzyltrimethylammonium (BTMA). The synthesis gel had the composition  $2.5\text{QAC}:\text{Al}_2\text{O}_3:12\text{SiO}_2:22\text{Na}_2\text{O}:0.64\text{K}_2\text{O}:200\text{H}_2\text{O}$ , where QAC denotes a quaternary ammonium cation.

**MAS NMR.** All samples were activated at  $400^\circ\text{C}$  under vacuum in Pyrex capsules designed to fit inside a zirconia MAS rotor. The catalyst was then charged with 30 wt %  $^{13}\text{C}$ -enriched methanol and the capsule sealed off under liquid nitrogen to prevent the onset of catalytic processes. The capsule could then be heated to the desired reaction temperature, quenched and placed in the NMR rotor to record  $^{13}\text{C}$  and  $^1\text{H}$  NMR spectra at ambient temperature.<sup>10,11</sup> Samples were spun at the magic angle at rates of up to 3 kHz. All spectra were recorded on a Bruker MSL-400 spectrometer.  $^{13}\text{C}$  spectra were measured using a double-bearing MAS probehead with zirconia rotors, and the  $^1\text{H}$  spectra a probehead acquired from Universität Leipzig.  $^{13}\text{C}$  spectra were recorded both with and without proton decoupling, but always without cross-polarization in order to keep the spectra quantitative. For experiments with high-power proton decoupling, 4-ms  $^{13}\text{C}$  pulses with a repetition time of 10 s and between 200 and 400 scans were used. Maximum  $T_1$  relaxation times were approximately 1.5 s which means that a 10-s recycle time is sufficient to provide quantitatively reliable spectra. The decoupler was gated off between experiments in order to prevent the nuclear Overhauser enhancement.  $^1\text{H}$  spectra were recorded using a Bloch decay with a  $90^\circ$  pulse of 4.5  $\mu\text{s}$  and a repetition time of 3 s.  $^1\text{H}$  signals were sufficiently intense to enable us to dispense with background suppression techniques.

(14) Mirth, G.; Lercher, J. A.; Anderson, M. W.; Klinowski, J. *J. Chem. Soc., Faraday Trans. 1* **1990**, *86*, 3039.

(15) Anderson, M. W.; Klinowski, J. *Chem. Phys. Lett.* **1990**, *172*, 275.

(16) Klinowski, M. W.; Anderson, M. W. *Magn. Reson. Chem.* **1990**, *28*, 68.

(17) Anderson, M. W.; Barric, P. J.; Klinowski, J. *J. Phys. Chem.* **1991**, *95*, 235.

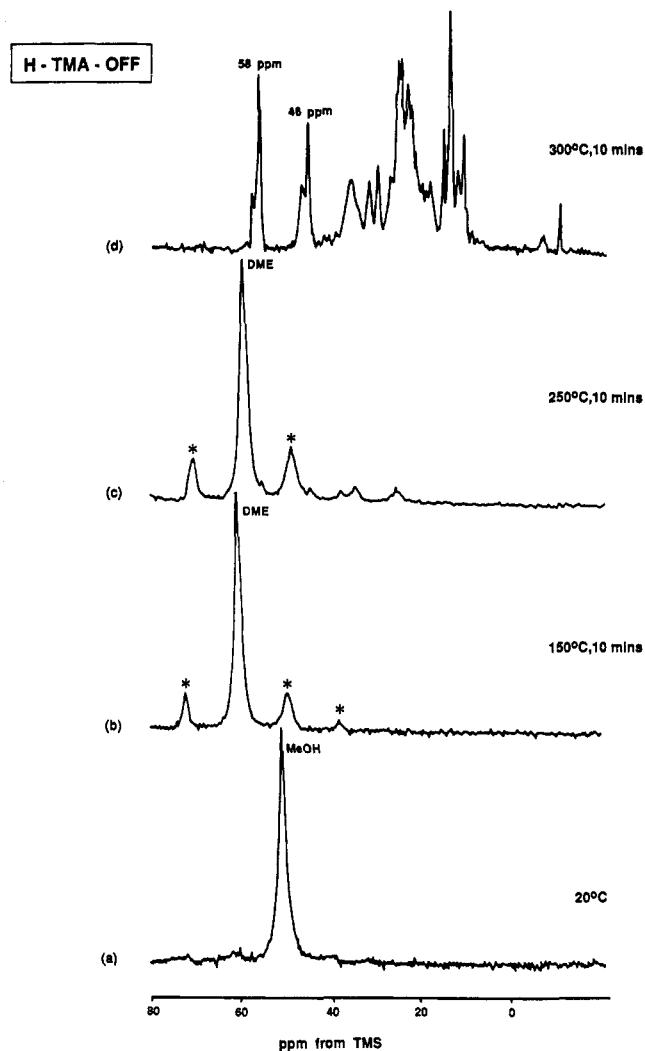


Figure 3.  $^{13}\text{C}$  MAS NMR spectra of the products of the conversion of methanol over zeolite H-TMA-OFF at (a) room temperature; (b)  $150^\circ\text{C}$ , 10 min; (c)  $250^\circ\text{C}$ , 10 min; (d)  $300^\circ\text{C}$ , 10 min. Asterisks denote spinning sidebands.

## Results

Figure 2 shows the  $^1\text{H}$  MAS NMR spectra of MeOH adsorbed on the four catalysts at room temperature. In all cases the methyl resonance is at 3.8 ppm from TMS, but the position of the hydroxyl resonance varies from 6.5 ppm on H-ZSM-34 and HTMA-OFF to 7.2 ppm on H-BTMA-OFF and 8.4 ppm on HDABCO-OFF.

Figure 3 gives the  $^{13}\text{C}$  spectra of the products of conversion over H-TMA-OFF. At room temperature there is a single resonance at 50.5 ppm, corresponding to MeOH. After heating at  $150^\circ\text{C}$  for 10 min all MeOH is converted into a single species with a  $^{13}\text{C}$  resonance of 61 ppm. The most likely assignment of this signal is to dimethyl ether (DME), but its origin in MeOSi groups cannot be excluded. Judging by the associated spinning sidebands (indicated by asterisks), the chemical shift anisotropy of this signal is at least 5 kHz. Further heating of the sample to  $250^\circ\text{C}$  produces a number of low-intensity resonances at 58, 47, 38, and 29 ppm. Finally, at  $300^\circ\text{C}$  a whole host of aliphatic hydrocarbon products are observed. Many of the resonances are very narrow, which indicates a high degree of molecular mobility. We assign the two resonances in the region 46–48 ppm and 58–60 ppm, neither of which is found in any other zeolitic system, to long-chain hydrocarbons.

At  $250^\circ\text{C}$  H-BTMA-OFF (Figure 4) and H-DABCO-OFF (Figure 5) effect complete conversion of MeOH to hydrocarbons, and the distribution of final products is almost identical. By contrast, H-ZSM-34 does not achieve complete conversion below  $300^\circ\text{C}$  (Figure 6). However, the final product distribution is

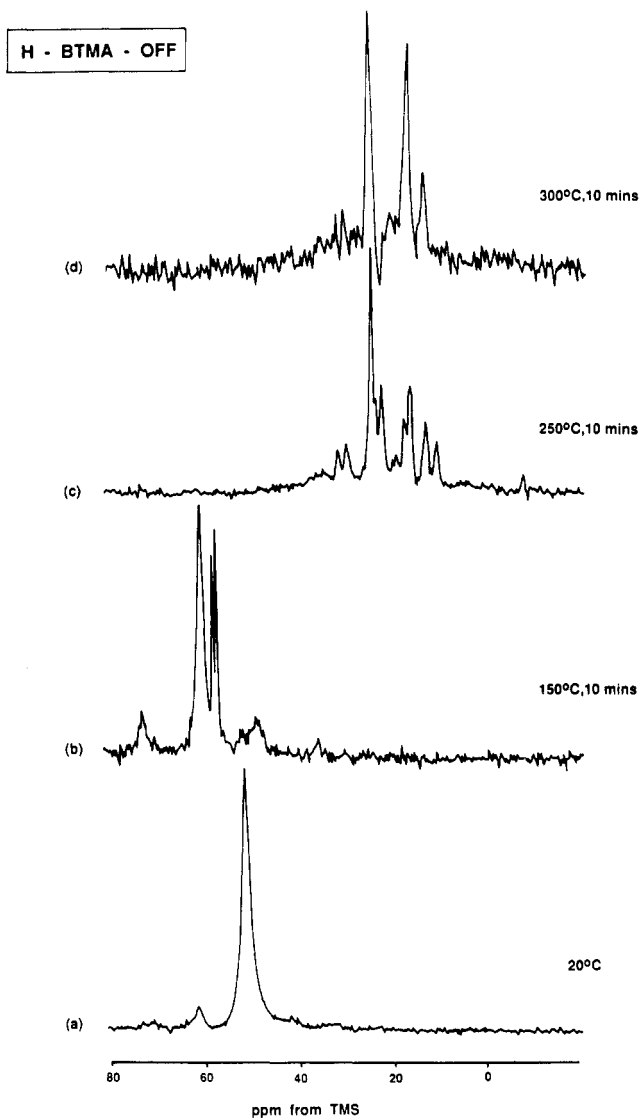


**Figure 4.**  $^{13}\text{C}$  MAS NMR spectra of the products of the conversion of methanol over zeolite H-BTMA-OFF at (a) room temperature; (b) 150  $^{\circ}\text{C}$ , 10 min; (c) 250  $^{\circ}\text{C}$ , 10 min; (d) 300  $^{\circ}\text{C}$ , 10 min.

similar, with hydrocarbons heavier than  $\text{C}_4$  being highly branched (see Table I). Considerably more methane is observed in HZSM-34 than in H-BTMA-OFF or H-DABCO-OFF. At 250  $^{\circ}\text{C}$  in H-ZSM-34 there are two sharp resonances at 60 and 59 ppm which are also observed, but in much lower abundance, in all the catalysts. These signals disappear at complete conversion. Figure 7 shows the  $^{13}\text{C}$  spectrum recorded without high-power proton decoupling for MeOH after complete conversion on HZSM-34 at 300  $^{\circ}\text{C}$ . The magnitude of J-coupling supports the spectral assignments given in Table I.

### Discussion

The structures of the zeolites offretite and erionite are closely related.<sup>5</sup> In offretite, one-dimensional channels outlined by 12-membered rings run unrestricted through the structure along the *c* direction. In erionite these channels are blocked every 15.2 Å by constrictions which create elliptical cages interconnected via 8-membered rings (Figure 1). Diffusion through these is therefore much more difficult. Intergrowths of offretite/erionite have varying degrees of main channel blocking, leading to varying degrees of channel tortuosity. The offretite/erionite system is thus useful for the study of the role of tortuosity in shape-selective catalysis.

The catalysts used in this work have already been characterized by X-ray and electron diffraction, HREM, solid-state  $^{29}\text{Si}$  and  $^{27}\text{Al}$  MAS NMR, and catalytic testing.<sup>7-9</sup> These studies have

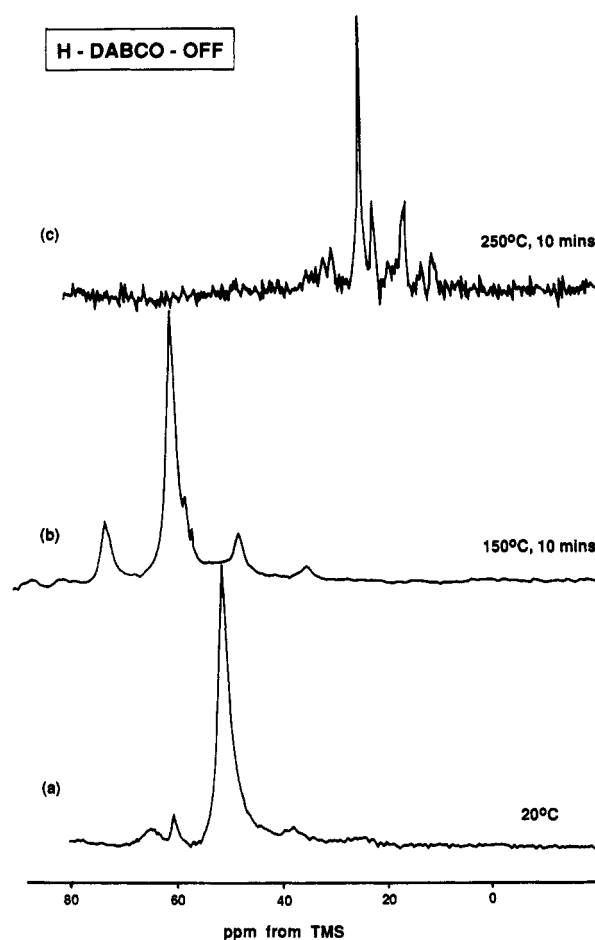


**Figure 5.**  $^{13}\text{C}$  MAS NMR spectra of the products of the conversion of methanol over zeolite H-DABCO-OFF at (a) room temperature; (b) 150  $^{\circ}\text{C}$ , 10 min; (c) 250  $^{\circ}\text{C}$ , 10 min.

**TABLE I: Conversion of Methanol over Zeolite H-ZSM-34 at 300  $^{\circ}\text{C}$ . Assignment of  $^{13}\text{C}$  NMR Resonances**

molecule	chemical shift, ppm from TMS				intensity, %
methane	-10.2				35
ethane	4.2				1
propane	16.1				21
butane	14.6	25.2			18
isobutane	23.2	25.2			9
pentane	15.0	22.6	35.2		4
isopentane	12.7	22.0	30.5	32.5	12

shown that the degree of erionite content decreases in the series H-DABCO-OFF, H-ZSM-34, H-BTMA-OFF, H-TMA-OFF. In other words, in H-DABCO-OFF channel blocking is the most frequent and in H-TMA-OFF the least frequent. However, it would be misleading to quote even approximate quantitative measures for their offretite or erionite content.

The Brønsted acidity of these catalysts can be assessed from the  $^1\text{H}$  chemical shifts of the MeOH hydroxyl group. As shown previously,<sup>17</sup> the greater the frequency of this resonance, the greater the proton-donating ability of the catalyst. H-ZSM-5 gives a resonance at 9.4 ppm, whereas the catalysts in this work have resonances between 6.5 and 8.4 ppm (Figure 2). This indicates the lower acidity of these catalysts compared with H-ZSM-5.

The effects on shape selectivity can be assessed by measuring the constraint index, defined as the ratio of branched to linear  $\text{C}_6$  molecules remaining after cracking an equimolar mixture of 3-methylpentane and *n*-hexane. The index reflects the degree of channel blockage and is lowest in H-TMA-OFF and highest in H-DABCO-OFF. In terms of selective conversion of methanol to ethylene and propylene, the zeolites with the most tortuous channels are the best. The most likely explanation is that the more tortuous channels "sieve out" the higher molecular weight and

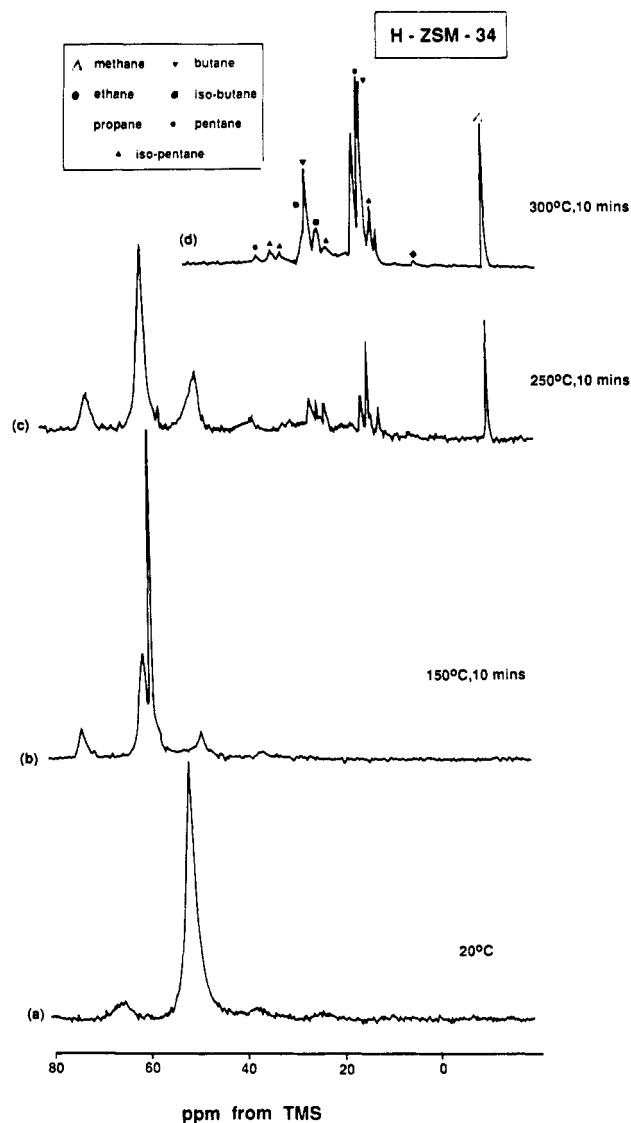
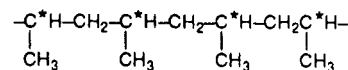


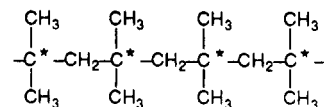
**Figure 6.**  $^{13}\text{C}$  MAS NMR spectra of the products of the conversion of methanol over zeolite H-ZSM-34 at (a) room temperature; (b) 150 °C, 10 min; (c) 250 °C, 10 min; (d) 300 °C, 10 min.

branched species while allowing the light olefins to diffuse more or less unhindered.

We were able to monitor not only the products which eventually escape from the zeolite but also those species which, on the time scale of the experiment, are trapped within the cavities. The presence of the latter species modifies the shape selectivity further: it is striking that long-chain polymeric hydrocarbons are formed in H-TMA-OFF, which is the most fault free and imposes no restriction to the polymerization of low molecular weight olefins. The magnitude of the  $^{13}\text{C}$  chemical shift shows that the polymers are highly branched: the resonance at ca. 46 ppm corresponds to the tertiary (starred) carbons in



groupings and that at ca. 58 ppm to the quaternary (starred) carbons in



groupings.

We are aware that the conversion of MeOH into activated  $\text{C}_1$  species is much slower than any of the subsequent steps. Moreover, oligomerization of  $\text{C}_2$  and  $\text{C}_3$  olefins will occur at lower temperatures, perhaps even during the quenching process. As the reaction capsule is closed, the degree of oligomerization will further depend on the partial pressure of the olefins. Although the present conditions are different from the conditions under which the reaction normally occurs, polymerization may provide an additional competitive reaction which reduces the selectivity of fault-free offretite-like catalysts to light olefins. This, in turn, is a further reason (apart from the benefits of tortuosity already discussed) for the use of more highly blocked channels for the production of light olefins. Similar polymerization is not found in H-BTMA-OFF, low in erionite, indicating that only a few blockages are required to prevent polymerization. It is difficult with the present data to assess the relative importance of tortuosity versus polymerization reactions for the selectivity of zeolite catalysts to light olefins. However, this new evidence should be taken into consideration when dealing with other one-dimensional zeolitic channel systems. In ZSM-5 no evidence was found for

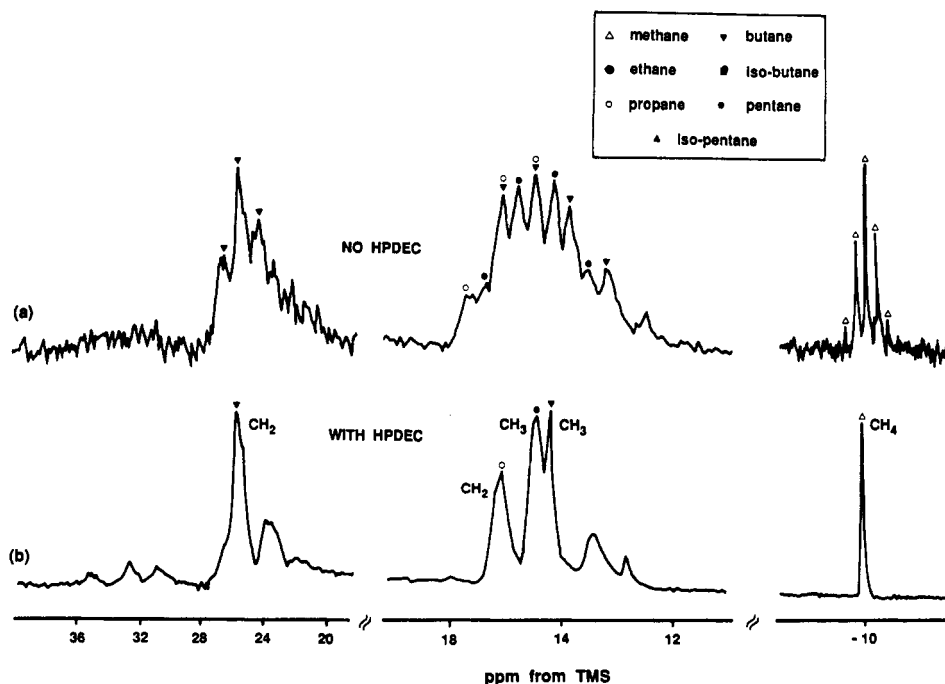


**Figure 7.**  $^{13}\text{C}$  MAS NMR spectra of conversion of methanol over H-ZSM-34 at 300 °C for 10 min recorded (a) without and (b) with high-power proton decoupling.

the buildup of long-chain hydrocarbons during the conversion of methanol. This might well be due to the narrower (10-membered) channels in ZSM-5, as opposed to 12-membered offretite channels, which might prevent the formation of branched polymer chains.

*Acknowledgment.* We are grateful to Shell Research, Amsterdam, for support.

Registry No. MeOH, 67-56-1.

## Orientalional Disorder of the Hydrogen Dihydroxide Anion, $O_2H_3^-$ , in Sodium Hydroxosodalite Dihydrate, $Na_8[Al_6Si_6O_{24}](OH)_2 \cdot 2H_2O$ : Single-Crystal X-ray and Powder Neutron Diffraction and MAS NMR and FT IR Spectroscopy

Michael Wiebecke,\* Günter Engelhardt, Jürgen Felsche, Paul Bernd Kempa, Peter Sieger,

Faculty of Chemistry, University of Konstanz, D-7750 Konstanz, Germany

Jürg Schefer,

Solid State Physics, Paul Scherrer Institute, CH-5232 Villigen PSI, Switzerland

and Peter Fischer

Laboratory for Neutron Scattering, ETH Zürich, CH-5232 Villigen PSI, Switzerland

(Received: March 15, 1991; In Final Form: July 25, 1991)

The crystal structure of sodium hydroxosodalite dihydrate,  $Na_8[Al_6Si_6O_{24}](OH)_2 \cdot 2H_2O$ , is cubic at 173 K with space group  $P43n$  ( $Z = 1$ ) and the cell constants  $a = 8.875$  (2) Å (X-ray),  $a = 8.87$  (5) Å (neutron, nondeuterated form), and  $a = 8.86$  (5) Å (neutron, deuterated form). The 1:1 aluminosilicate framework is a strictly alternating arrangement of corner-sharing  $AlO_4$  and  $SiO_4$  tetrahedra. Each  $[4^6 6^8]$  polyhedral cage is occupied by four Na cations, located close to oxygen atoms of six-membered rings of the framework, and, near the center, by a 6-fold or 12-fold orientationally disordered hydrogen dihydroxide anion,  $O_2H_3^-$ , of point symmetry 2 ( $C_2$ ) with a very strong central hydrogen bond  $O \cdots H \cdots O$  with  $O \cdots O$  distances at 2.36 (4) Å (nondeuterated powder sample) and 2.28 (4) Å (deuterated powder sample). The hydrogen atom in the central hydrogen bond is probably (dynamically) disordered between two positions near the 2-fold axis, i.e. the anion is probably of the type  $[HO \cdots (H,H) \cdots OH]^-$ . No hydrogen bonding exists between the terminal OH groups of the anion and framework oxygen atoms. The structure model is in line with the  $^1H$  MAS NMR spectrum with chemical shifts at 16.3 ppm (central hydrogen atom) and  $-0.1$  ppm (terminal hydrogen atoms) and the mid IR spectra of the nondeuterated and deuterated forms. The structural formula  $[Na_4(O_2H_3)]_2[Al_6Si_6O_{24}]$  is suggested for hydroxosodalite dihydrate. Reversible structural-phase transitions were verified by DSC measurements which showed two heat effects at  $150 \pm 1$  K and  $154 \pm 1$  K for nondeuterated, but only one heat effect at  $150 \pm 1$  K for deuterated samples. Structure chemical considerations suggest that a recently published orthorhombic crystal structure for the low-temperature phase may be incorrect.

### Introduction

Sodalites  $M_8[T_{12}O_{24}]X_2$  are host-guest compounds with three-dimensional 4-connected host structures built up of corner-sharing  $TO_4$  tetrahedra with  $T = Si^{4+}, Ge^{4+}, Al^{3+}, Ga^{3+}$ , etc.<sup>1</sup> These frameworks are unique in that only one kind of polyhedral cavity, the  $[4^6 6^8]$  truncated octahedron (one of the five space-filling Federov solids), is formed in which a large variety of different cationic ( $M = Li^+, Na^+, K^+$ , etc.) and anionic ( $X = OH^-, Cl^-, NO_2^-, ClO_4^-$ , etc.) guest species may be enclathrated. Depending on composition, sodalites possess photochromic, cathodochromic, and ion-conducting properties, show redox or decomposition reactions inside the cages ("intracage chemistry"), and have very recently attracted considerable attention as matrices for metal and semiconductor clusters and extended superclusters in the quantum size regime ("nanocomposites").<sup>2</sup> Because the truncated octahedron (also known as sodalite cage or  $\beta$ -cage) is a polyhedral building unit of the industrially important zeolites A (LTA topology) and X and Y (FAU), sodalites have also been regarded as model substances for studying pure  $\beta$ -cage properties.<sup>3-5</sup> This

is especially true for the aluminosilicate hydrosodalites  $Na_{6+x}[Al_6Si_6O_{24}](OH)_x \cdot nH_2O$ , which may be divided into two end-member series, the nonbasic hydrosodalites with  $x = 0, n \leq 8$ , and the basic hydrosodalites (hydroxosodalites) with  $x = 2$  and  $n \leq 4$ .<sup>4,5</sup> The  $H_2O$  content of hydroxosodalite hydrates  $Na_8[Al_6Si_6O_{24}](OH)_2 \cdot nH_2O$  has still been in debate until very recently, when it was shown experimentally by Engelhardt et al.<sup>6</sup> that with the commonly used synthesis methods only  $Na_8[Al_6Si_6O_{24}](OH)_2 \cdot 2H_2O$  is formed as the primary product; all formerly reported compositions with  $x = 2$  and  $n > 2$  do not exist but are mixtures of  $Na_8[Al_6Si_6O_{24}](OH)_2 \cdot 2H_2O$  and  $Na_6[Al_6Si_6O_{24}] \cdot 8H_2O$ , due to partial exchange of NaOH against  $H_2O$  during washing procedures.

Structure and dynamics of the guest species in hydroxosodalite hydrates  $Na_8[Al_6Si_6O_{24}](OH)_2 \cdot nH_2O$  have been studied by  $^1H$  and  $^{23}Na$  NMR spectroscopy,<sup>7</sup> mid and far IR spectroscopy,<sup>8</sup> as well as single-crystal X-ray<sup>9,10</sup> and single-crystal neutron dif-

(4) Felsche, J.; Luger, S. *Ber. Bunsenges. Phys. Chem.* 1986, 90, 731.

(5) Felsche, J.; Luger, S. *Thermochim. Acta* 1987, 118, 35.

(6) Engelhardt, G.; Felsche, J.; Sieger, P. *J. Am. Chem. Soc.*, in press.

(7) Galitskii, V. Yu.; Grechushnikov, B. N.; Ilyukhin, V. V.; Belov, N. V. *Sov. Phys. Dokl.* 1974, 19, 111. Detinich, V. A.; Kriger, Yu. G.; Galitskii, V. Yu. *Sov. Phys. Crystallogr.* 1988, 33, 917.

(8) Godber, J.; Ozin, G. A. *J. Phys. Chem.* 1988, 92, 4980.

(1) Depmeier, W. *Acta Crystallogr., Sect. B* 1984, B40, 185. Hassan, I.; Grundy, H. D. *Acta Crystallogr., Sect. B* 1984, B40, 6.

(2) Ozin, G. A.; Kuperman, A.; Stein, A. *Angew. Chem.* 1989, 101, 373.

(3) Smith, J. V. *Chem. Rev.* 1988, 88, 149.